D. V. Bandourin[1], V. F. Konoplyanikov[2], N. B. Skachkov[3]

ON THE POSSIBILITY OF DISCRIMINATION BETWEEN π^0-, η-, ω-, K_s^0-MESONS AND A PHOTON BASED ON THE CALORIMETER INFORMATION IN THE CMS DETECTOR

[1]E-mail: dmv@cv.jinr.ru
[2]E-mail: kon@cv.jinr.ru
[3]E-mail: skachkov@cv.jinr.ru

1. Introduction.

This work is a continuation of our previous publications on the study of "$\gamma +$ jet" events at LHC energies [1] – [8]. In these papers it was shown that a process of a direct photon production (with $P_t^{\gamma} > 40 \; GeV/c$) in association with one jet, caused mainly by Compton-like $qg \rightarrow \gamma + q$ and annihilation subprocesses $q\bar{q} \rightarrow \gamma + g$, has a significant background due to other QCD processes that contain high P_t final state photons originating from π^0, η, K_s^0 and ω mesons decays (see [7]). The former subprocess, as it was pointed in [9], can be used at LHC for studying the gluon density in a proton in the reaction of inclusive direct photon production and in the "$\gamma + jet$" events ([8], [10], [11]). As for the decay channels of the abovementioned mesons (see Table 1 with the PDG data [13] of branching ratios), we shall consider first the neutral decay channels ($\pi^0 \rightarrow 2\gamma$; $K_s^0 \rightarrow 2\pi^0$; $\eta \rightarrow 3\pi^0$ and 2γ) as the next most important background source (especially with increasing a signal photon energy) after the processes with a hard radiation of photons from quarks, i.e. bremsstrahlung photons (see [7]).

Table 1: Decay modes of π^0, η, K_s^0 and ω mesons.

Particle	Br.(%)	Decay mode
π^0	98.8	$\gamma\gamma$
	1.2	$\gamma e^+ e^-$
η	39.3	$\gamma\gamma$
	32.2	$\pi^0\pi^0\pi^0$
	23.0	$\pi^+\pi^-\pi^0$
	4.8	$\pi^+\pi^-\gamma$
K_s^0	68.6	$\pi^+\pi^-$
	31.4	$\pi^0\pi^0$
ω	88.8	$\pi^+\pi^-\pi^0$
	8.5	$\pi^0\gamma$

We shall study a question of what level of accuracy can be achieved in suppression of the contribution from these neutral decay channels if we shall confine ourselves only to the information from the CMS electromagnetic calorimeter (ECAL). Possible use of preshower detector information is not considered here as it was a subject of another publication [12].

Another group of decay channels that contain charged pions in the final state is less difficult to be suppressed. As will be shown below, their contribution to the background can be discriminated with a good efficiency on the basis of the hadronic calorimeter (HCAL) data.

The results presented here are obtained from the simulation with the GEANT

1

based package CMSIM [1]. We carried out a series of simulation runs including:
(1) four particle types: single photons γ and π^0, η, K_s^0 mesons;
(2) six E_t values for each of these particles: $20, 40, 60, 80, 100$ and $200\ GeV$;
(3) two pseudorapidity regions: $0.4 < \eta < 1.0$ (Barrel) and $1.6 < \eta < 2.0$ (Endcap).
About $4000 - 5000$ single-particle events were generated for each E_t, η interval and for each type of a particle.

2. Neutral decay channels.

To separate the single photon events in the ECAL from the events with photons produced in the neutral decay channels of π^0, η, K_s^0 and ω mesons, two variables which characterize the spatial distribution of E_t deposition in both cases were used:

    1. E_t deposited inside the most energetic crystal cell in the ECAL E_{tmax}^{cell};
    2. The quantity D_w that characterizes E_t spatial distribution inside the 5×5 crystal window around the most energetic crystal cell (see below).

    The showers produced in ECAL crystal cells by the single photon is concentrated in a $5{\times}5$ array of crystals centered on the crystal with the maximum signal (see [16]). Another picture is expected for the multiphoton final state arising from the meson decay through the intermediate π^0 states that would cause different spatially separated centers of final state photon production. In this case the spatial distribution of E_t deposited in such a shower is also more likely to be different from that one produced by a single photon.

    Let us define the coordinates of the ECAL shower center of gravity (gc) in the $\eta - \phi$ space according to formula:

$$\eta_{gc} = \left(\sum_{i=1}^{N \times N} \eta_i E_t^i \right) / \left(\sum_{i=1}^{N \times N} E_t^i \right); \quad \phi_{gc} = \left(\sum_{i=1}^{N \times N} \phi_i E_t^i \right) / \left(\sum_{i=1}^{N \times N} E_t^i \right) \quad (1)$$

The sum in formula (1) runs over ECAL crystal cells [2] forming the $N \times N$ window that contain a shower with the most energetic cell in the center. Here E_t^i is E_t deposited inside the ith crystal cell belonging to the shower.

    The obtained distributions of E_t deposited in ECAL by single photon, η and π^0 mesons having four initial values of $E_t = 20, 40, 60$ and $100\ GeV$ are shown in Fig. 1 as a function of the distance counted from the center of gravity R_{gc}. One can see from Fig. 1 that about 96% of the total photon E_t deposited in ECAL, i.e. Et_tot, fits into the radius $R_{gc} = 0.02$ and practically all its energy is contained inside $R_{gc} = 0.045$. From the same pictures we can conclude that for all meson the total E_t of showers

---

[1] The results in Section 2 and 3 of this Appendix are obtained with CMSIM versions 111 and 116 respectively.
  [2] (with a cell size of $0.0175{\times}0.0175$)

is mainly contained inside the 5×5 crystal cell window having the size of one CMS HCAL tower. So, in formula (1) we can put with a good accuracy $N = 5$. We also observe from this figure that the difference in spectra for single photons and pions decreases with growing E_t and practically disappears at $E_t = 100 \ GeV$, while the difference of the distributions caused by η mesons from those for single photons can still be seen at $E_t = 60$ and $100 \ GeV$.
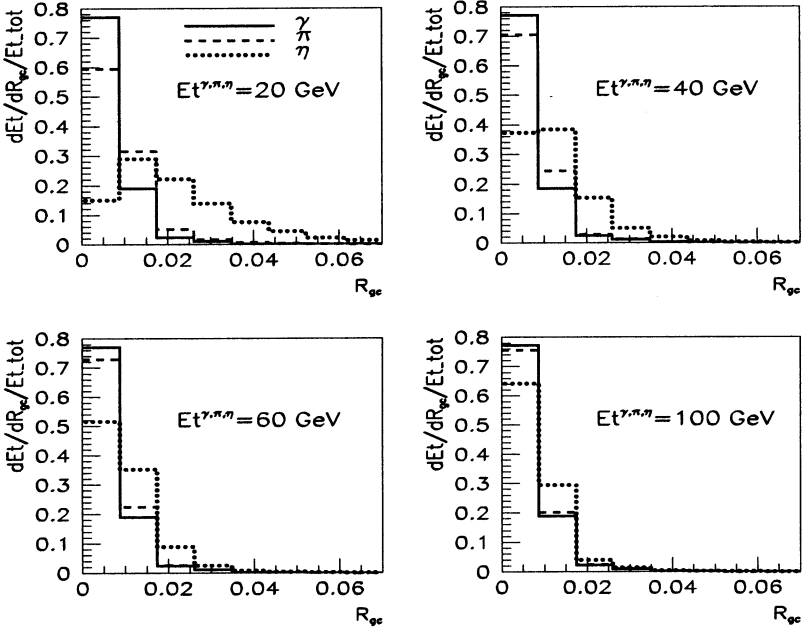

Figure 1: The normalized $dEt/dR_{gc}/Et\_tot$ distribution over R_{gc} of the showers produced in ECAL by π^0, η mesons and single photons γ having $E_t = 20, 40, 60$ and $100 \ GeV$.

For our further needs we introduce another useful variable. Let us consider the distance r_i of the ith cell from the center of gravity of the electromagnetic shower in ECAL, i.e.

$$r_i = ((\phi_i - \phi_{gc})^2 + (\eta_i - \eta_{gc})^2)^{1/2}, \qquad (2)$$

where (η_i, ϕ_i) are coordinates of the center of the ECAL crystal cell. The distances r_i of each crystal cell can be used to introduce a new useful quantity (that effectively takes into account the contribution of energetic cells far from the center of gravity):

$$D_w = \left(\sum_{i=1}^{25} r_i E_t^i \right) / \left(\sum_{i=1}^{25} E_t^i \right). \qquad (3)$$

3

For illustration, we present the results of CMSIM simulation with $E_t^{\gamma/mes} = 40\ GeV$ ($mes = \pi^0, \eta$) in Figs. 2 and 3. These figures contain the normalized distributions of E_{tmax}^{cell} and D_w that characterize the showers produced by the products of η meson (Fig. 2) and π^0 meson (Fig. 3) decays. The analogous E_{tmax}^{cell} and D_w distributions in the showers produced by a single photon are also shown there for comparison.
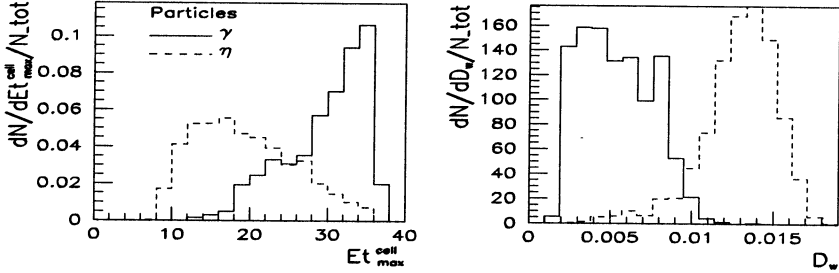
Figure 2: The normalized distributions of the number of events over D_w and E_{tmax}^{cell} for the single photons (γ) and for ECAL showers originating from η mesons (η) having $E_t = 40\ GeV$.
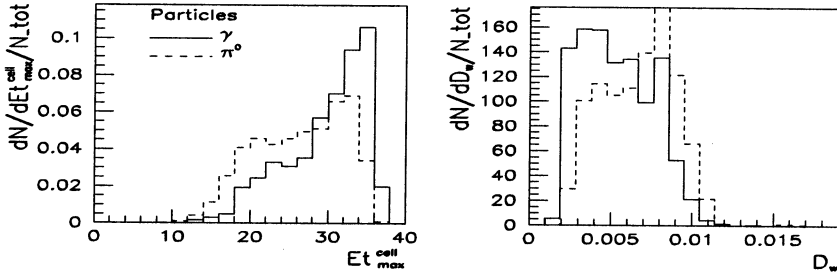
Figure 3: The normalized distributions of the number of events over D_w and E_{tmax}^{cell} for the single photons (γ) and for π^0 mesons (π^0) having $E_t = 40\ GeV$.

One can easily see that the η meson shower spectrum over D_w is strongly different from the one of the photon. The range of E_{tmax}^{cell} values where the η meson background makes a small contribution ($E_{tmax}^{cell} \geq 28\ GeV$) is also clearly seen in Fig. 2. From the result of the simulation we conclude that 90% of the signal photon events at $E_t^{\gamma/mes} = 40\ GeV$ are concentrated in the regions $D_w \leq 0.0088$ and $E_{tmax}^{cell} \geq 23\ GeV$.

So, the E_{tmax}^{cell} and D_w spectra of the η meson can be effectively used for separation of the background and the signal events because the region of their overlapping becomes much smaller as compared with Fig. 1.

We call the way of separation of signal and background events based on the spectra differences over the 1st variable E_{tmax}^{cell} as "Et_max" criterion and over the 2nd variable D_w as "D_w" criterion.

The situation is much worse in the case of π^0 showers as is seen in Fig. 3 where the spectra of π^0 practically overlap with the spectra of photon.

The neutral pion rejection efficiencies $R_{eff}^{\pi^0}$ (against direct photons) [3] obtained basing on D_w criterion for different values of E_t^{γ/π^0} are given in Table 2 as a function of a chosen value of single photon selection efficiencies (in %) ϵ_{eff}^{γ}= 80, 85, 88 and 90 %. The second line in this table "$E_t^{\gamma/\pi^0} = 40\ GeV$" corresponds to the plots in Fig. 3. We see from this table that $R_{eff}^{\pi^0}$ grows almost twice by decreasing ϵ_{eff}^{γ} from 90% to 80%.

Table 2: Neutral pion rejection efficiencies $R_{eff}^{\pi^0}$ (%) obtained from CMSIM simulation by application of D_w criterion for five E_t values of single γ and π^0 and for different values of single γ selection efficiencies $\epsilon_{eff}^{\gamma} = 80-90\%$. $0.4 < \eta^{\gamma,\pi} < 1.0$.

E_t^{γ/π^0} (GeV)	photon selection efficiencies ϵ_{eff}^{γ}			
	80%	85%	88%	90%
20	71	64	59	54
40	38	32	25	22
60	33	26	20	17
80	29	21	17	14
100	25	20	16	13

The rejection percentages of events with π^0 for each of the criteria Et_max and D_w are given in Fig. 4 for different meson E_t [4].

The analogous rejection curves obtained for the η and K_s^0 meson neutral channels (for the fixed value of single photon selection efficiency $\epsilon_{eff}^{\gamma} = 90\%$) are presented in Fig. 5 (Et_max criterion) and in Fig. 6 (D_w criterion) for the interval $20 \leq E_t \leq 200\ GeV$.

By comparing Fig. 5 for the case of η meson and Fig. 4 we see that for one and the same $\epsilon_{eff}^{\gamma}(= 90\%)$ and the same rejection criterion Et_max the π^0 rejection efficiency $R_{eff}^{\pi^0}$ becomes less than 30% at $E_t = 30\ GeV$ while the η meson rejection efficiency drops to the same level of 30% only at $E_t \geq 90\ GeV$. It is also seen that

---

[3]The rejection efficiency is defined as a ratio of the number of background events discarded by the cut, taken for a given value of signal selection efficiency ϵ_{eff}^{γ}, to the total number of background events.

[4]The rejection factors for the Endcap are found to be in the correspondence with those of [15] (without preshower) if one takes into account the fact that in Fig. 4 the rejection powers are averaged over the entire $1.6 < \eta < 2.0$ range.

D_w criterion works a bit better than Et_max one for the Barrel region ($0.4 < \eta < 1.0$).

In spite of a difficulty of neutral pion background separation from single photon signal it is worth reminding that, as it was already mentioned in [7], the π^0 background events contribution (as well as the contribution from η, ω and K_s^0 events), left after
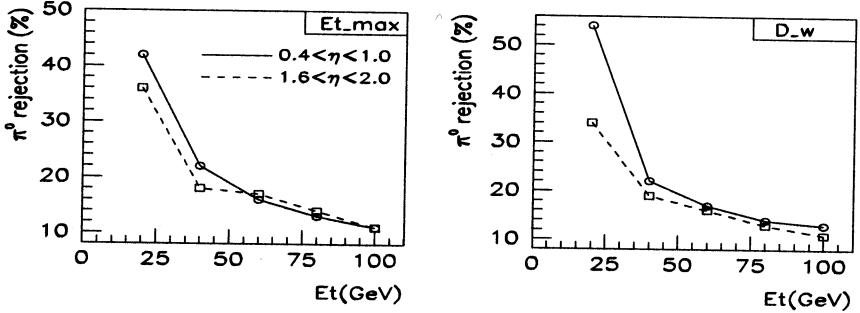

Fig. 4: π^0 rejection efficiencies for Et_max and D_w criteria ($\epsilon_{eff}^\gamma = 90\%$).
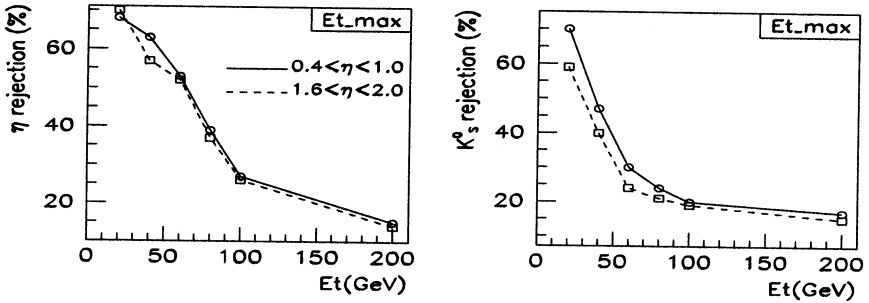
Fig. 5: η and K_s^0 rejection efficiencies for $\epsilon_{eff}^\gamma = 90\%$. Neutral decay channels only. Et_max criterion.
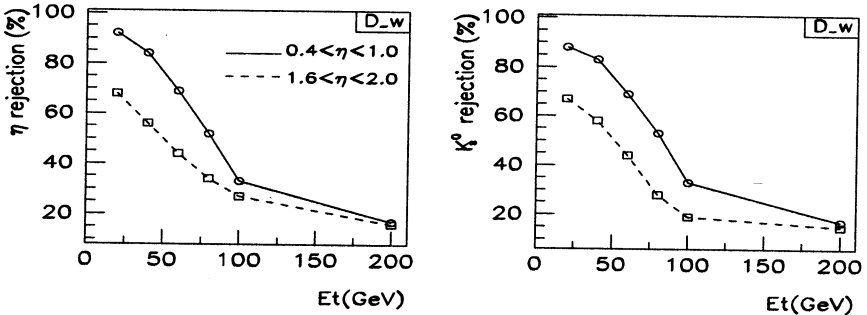

Fig. 6: η and K_s^0 rejection efficiencies for $\epsilon_{eff}^\gamma = 90\%$. Neutral decay channels only. D_w criterion.

6

the cuts chosen in [3] and [7] decreases with E_t growing faster than the "$\gamma - brem$" contribution. By this reason the bremsstrahlung photon background is more dangerous than that one from π^0 events. It was also shown in [7] that the contribution to the total background from the events containing ω meson as a candidate to the direct photon is less than $1 - 2\%$. Besides a part of the neutral decay channels is only 8.5% (Table 1). That is why we have not considered in this section the rejection possibility of the ω mesons decaying via neutral decay channels.

3. Charged decay channels.

Now let us return to the second group of the mesons decay channels that have charged daughter particles in the final state (28% of η, 68.6% of K_s^0 and 88.8% of ω meson decays; see Table 1).

We have studied the angle separation between the charged pions originating from ω and η mesons and the neutral pion (like in a case $\eta, \omega \to \pi^+\pi^-\pi^0$) or photon ($\eta \to \pi^+\pi^-\gamma$) produced in the same meson decay. For this aim the simulation of 1 million pp events at $\sqrt{s} = 14\ TeV$ was carried out using PYTHIA 5.7 with the set of all QCD and SM subprocesses having big cross sections. The minimal P_t of hard $2 \to 2$ subprocess, i.e. $\hat{p}_\perp^{min} \equiv CKIN(3)$ parameter in PYTHIA, was taken to be $\hat{p}_\perp^{min} = 40\ GeV/c$. The corresponding spectra normalized to unity are presented in Figs. 7 and 8 for $E_t^{\omega,\eta} \geq 30\ GeV$ separately for the charged pions with maximal and minimal values of E_t. One can see (Fig. 7) that the charged pion deflects from the π^0 direction in the hadronic decay of ω by the angle $\Delta\theta = 0.4 - 0.5°$ and by the angle $\Delta\phi = 1.0 - 1.3°$, on the average (the ϕ size of one crystal cell is about $\Delta\phi = 1°$). The corresponding averaged deflections in the abovementioned hadronic decays of η meson are by $\Delta\theta = 0.2°$ and by $\Delta\phi = 0.5°$ (see Fig. 8). Thus, from the distributions shown in Figs. 7 and 8 we may conclude that practically in all events the charged pions enter the same 5×5 ECAL crystal window as $\pi^0(\gamma)$ does and they may deposit partially their energy in HCAL towers behind the ECAL cells that register the $\pi^0(\gamma)$ signal [5]. The appearance of the corresponding signal in HCAL (see below for details of CMSIM simulation) may allow, in principle, to reject the events with hadronic background.

The E_t spectra of the charged pions originally produced in these channels were also studied using PYTHIA. They are presented in Fig. 9 for parent η, K_s^0 and ω mesons having $E_t = 40\ GeV$ separately for charged pions with maximal E_{tmax}^π and minimal E_{tmin}^π in the decay event. We see that the E_{tmax}^π distribution spectra for

---

[5]These results, strictly speaking, are valid only on the PYTHIA level of simulation and may be slightly modified while taking into account the magnetic field effect in full GEANT simulation with CMSIM.

mesons having $E_t = 40\ GeV$ start at about $17 - 18\ GeV$ for $\pi^{\pm}$ from K_s^0 decays and at about $5 - 6\ GeV$ for $\pi^{\pm}$ produced in decays of η and ω mesons.

So far we were discussing the spectra obtained at the level of PYTHIA simulation without the account of detector effects. In Fig. 10 we present two spectra obtained after CMSIM simulation of the calorimeter response to the propagation of charged pions in the CMS detector (the complete CMS setup was used). They correspond to the case of charged pions having $E_t = 5\ GeV$ and pseudorapidity η equal to 0.4 and 1.7. The spectra are normalized to the total number of events and describe the distribution of transverse energy deposited in the HCAL ("Et_dep"). They are built using 2000 CMSIM simulated events with a single charged pion for each η direction.
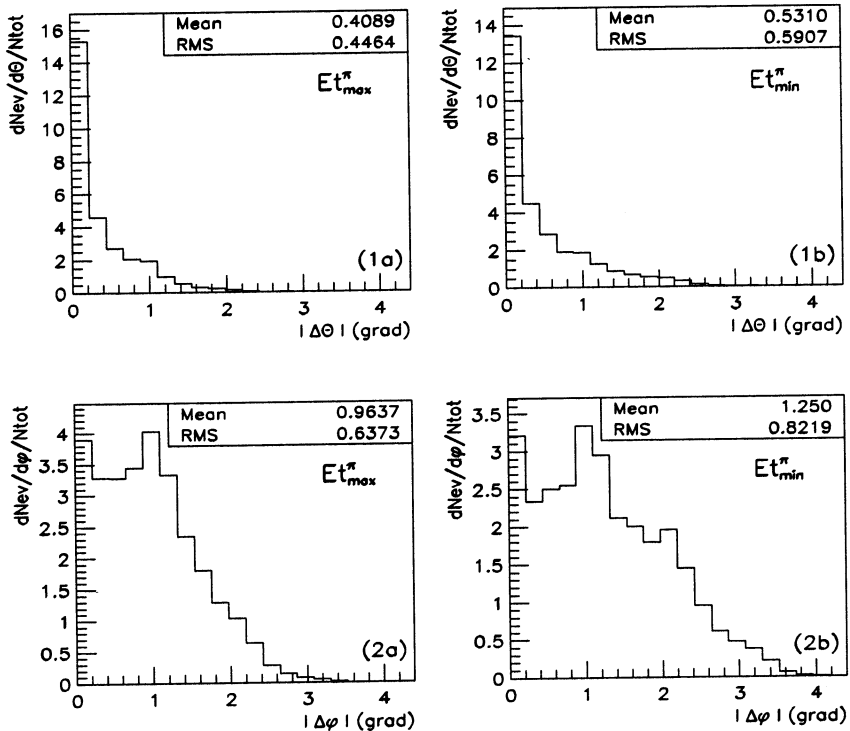

Figure 7: Absolute values of the difference in the θ and ϕ angles between $\pi^{\pm}$ and photons or π^0 originated from the $\omega \to \pi^+\pi^-\pi^0$ decay. Plots *1a (1b)* and *2a (2b)* correspond to the spectra over the angles between π^0 and the charged pion with the maximal(minimal) E_t^{π} in the decay channel.

One can see from Fig. 10 that even a single charged pion with $E_t = 5\ GeV$ has enough deposited energy to produce a noticeable signal in the HCAL in more than 90% of events. In decays mentioned in Table 1 the charged mesons are produced in pairs. The E_t spectra of the meson having the largest E_t in this pair start at $E_t^{\pi}{}_{max} \geq 5\ GeV$ as may be seen from Fig. 9. So, one can expect that at least 90% of this background may by rejected by measuring the HCAL signal.

As we noted above, in reality we shall have a combined contribution of two charged pions to the 5×5 ECAL crystal cell window in one decay (see Figs. 7 and 8) and, thus, to HCAL towers behind it. The following CMSIM simulations were carried out to investigate this contribution. First we considered the η meson decay
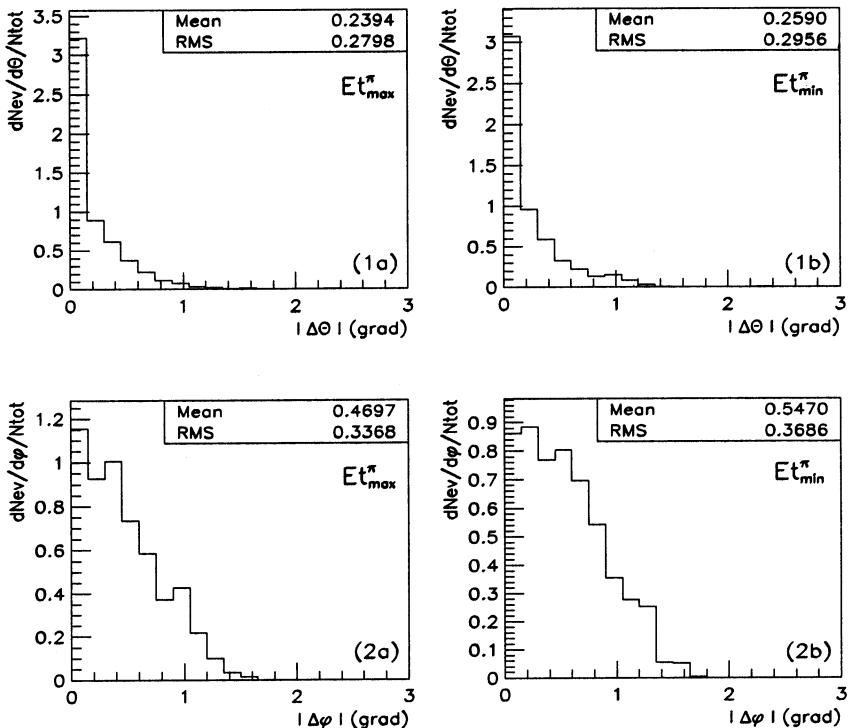

Figure 8: Absolute values of the difference in the θ and ϕ angles between charged $\pi^{\pm}$ and γ originated from the $\eta \rightarrow \pi^+\pi^-\gamma$ decay as well as between $\pi^{\pm}$ and π^0 from the $\eta \rightarrow \pi^+\pi^-\pi^0$ decay. Plots $1a$ ($1b$) and $2a$ ($2b$) correspond to the spectra over the angles between π^0 or γ and charged pion with maximal (minimal) E_t^{π} in the decay channel.
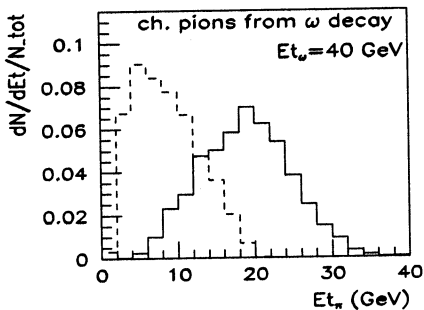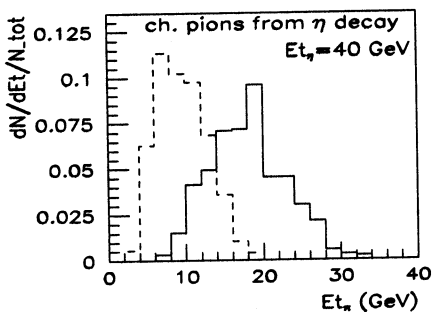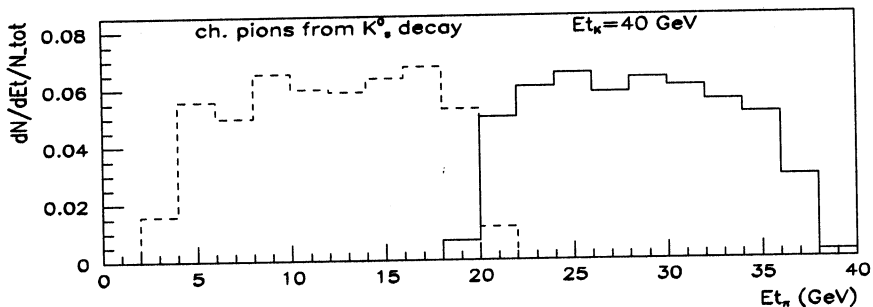
Figure 9: E_t spectra of charged pions from K_s^0, η and ω meson decays. Dashed and solid lines correspond to $E_{t\,min}^\pi$ and $E_{t\,max}^\pi$ distributions respectively.
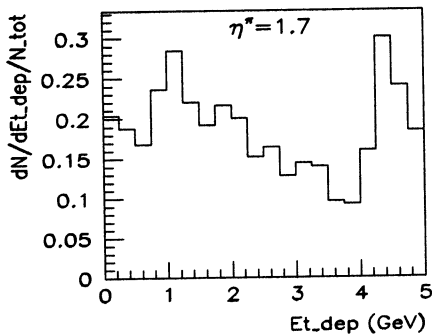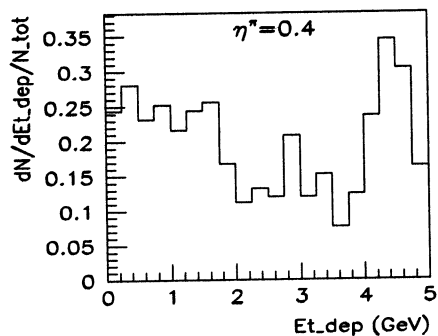

Figure 10: E_t deposited in the HCAL by charged pions with initial $E_t = 5\,GeV$. The left-hand plot corresponds to the Barrel region, the right-hand one corresponds to the Endcap region.

as a typical example. To examine in what way the charged mode of η meson decay can fake the signal photon we forced η meson to decay only through the charged channels ($\eta \to \pi^+\pi^-\pi^0$, $\pi^+\pi^-\gamma$) with the pseudorapidities $\eta = 0.4$ (Barrel region) and $\eta = 1.7$ (Endcap region). Three ranges of E_t values of the initial η meson were chosen (for both pseudorapidity values): $E_{t_{init}}^{\eta} = 40 \div 60$, $60 \div 80$ and $80 \div 100$ GeV. By about $5000 - 7000$ of the single η meson events for each η direction and E_t interval were generated for this aim (again with the complete setup of the CMS detector).

Since we want here to separate the η meson background basing on the presence of its decay hadronic products around a photon or a neutral pion (see Table 1), we shall apply here the isolation criteria formulated in [3]. It turned out that in the abovementioned generated samples of η meson events the number of events with the transverse energy inside the 5×5 ECAL crystal cell window $E_{t_{ECAL}}^{5\times5} \geq 40$ GeV is not quite sufficient for our analysis. As a good approximation to the value declared in [3] ($P_t^{\gamma} > 40$ GeV/c) we have chosen here $E_{t_{ECAL}}^{5\times5} \geq 35$ GeV as a lower cut.

The spectra of the hadronic transverse energy deposited in HCAL towers behind the 5×5 ECAL crystal cell window [6] $E_{t_H}^{sum}$ are given in plots (a1), (b1) and (c1) of Figs. 11 and 12 for the Barrel and the Endcap, respectively, for three abovementioned E_t ranges. In these plots $E_{t_H}^{sum}$ is defined as the sum of the transverse energies E_t^i

$$E_{t_H}^{sum} = \sum_i E_t^i \tag{4}$$

deposited in each ith HCAL tower fired by $\pi^{\pm}$ showers. No events were found with E_t deposited in HCAL with values $E_{t_H}^{sum} \leq 0.5$ GeV. In the intervals of $E_{t_{init}}^{\eta} = 40 \div 60$ and $60 \div 80$ GeV only about $0.1 - 0.2\%$ of the events, which have passed the cut $E_{t_{ECAL}}^{5\times5} > 35$ GeV, have $E_{t_H}^{sum} \leq 1$ GeV. No events with the $Et_H^{sum} \leq 1$ GeV were found for the $E_{t_{init}}^{\eta} = 80 \div 100$ GeV for both values $\eta = 0.4$ and 1.7.

Let us remind that we have chosen in [3] the value of the isolation cone radius around a γ^{dir}-candidate to be $R_{isol}^{\gamma} = 0.7$. It is useful to look for what radius of the hadronic energy shower from the η meson decay may be in reality. For this aim we calculate the value of $F_H(R) \equiv E_{t_H}^{sum}(R)/E_{t_{ECAL}}^{5\times5}$. The value $E_{t_H}^{sum}(R)$ differs from $E_{t_H}^{sum}$ defined by (4) by including into the sum only those towers that fits into the circle of some radius $R(\eta, \phi)$ counted from the most energetic ECAL crystal cell of the described above 5×5 ECAL crystal window, i.e.

$$E_{t_H}^{sum}(R) = \sum_{i \in R} E_t^i. \tag{5}$$

The dependence of $F_H(R)$ on this radius describes the E_t saturation of the space around the most energetic ECAL cell in 5×5 ECAL crystal window. This dependence

---

[6] containing $E_{t_{ECAL}}^{5\times5} \geq 35$ GeV

is shown in Fig. 13 by dashed line for three ranges of the initial transverse energies and two values of η. The quantity reaches the saturation values in the range of $R(\eta, \phi) \approx 0.3 - 0.4$, that has a meaning of a real radius of the hadronic energy deposition in HCAL for the single η meson decay. This value agrees with the value of $R_{isol}^{\gamma} = 0.7$ chosen in [3].

Now let us look what size of an additional E_t would be added into the isolation cone by the energy of charged pions deposited in ECAL cells surrounding the 5×5 ECAL crystal window (containing $E_{tECAL}^{5\times5} \geq 35~GeV$). Let us define the value of E_{tE+H}^{sum-} as the the scalar sum of E_t deposited inside the calorimeter ECAL+HCAL cells around the ECAL 5×5 crystal cell window (i.e. with a subtraction of E_t deposited inside the ECAL 5×5 crystal cell window itself):

$$E_{tE+H}^{sum-} = \sum_{i \in ECAL+HCAL} E_t^{i} - E_{tECAL}^{5\times5}. \tag{6}$$

Plots (a2), (b2) and (c2) in Figs. 11 and 12 include the spectra of E_t deposited in the ECAL+HCAL calorimeter cells that are beyond the 5×5 ECAL crystal cell window containing the most energetic crystal cell in its center, but within the radius $R(\eta, \phi) = 0.7$ counted from the center of this cell. They are given again for three different ranges of $E_{t init}^{\eta}$ and two values of pseudorapity $\eta = 0.4$ and 1.7. We see that all spectra in Figs. 11 and 12 steeply go to zero in the region of small E_t values. It allows to reduce the background from the charged η meson decays by limiting E_t deposited in the ECAL+HCAL cells within the radius $R(\eta, \phi) = 0.7$. One can see from the right-hand side columns of Figs. 11 and 12 that there are no events with E_t less than 2 GeV for the entire range of $E_{t init}^{\eta}$ $40 \div 100~GeV$ and both pseudorapidity values. This fact partially explains our choice of the direct photon isolation cut in [3] with $E_t^{isol} \leq 2~GeV/c$.

Let us introduce another variable $F_{E+H}(R)$ which has a meaning of the ratio of $E_{tE+H}^{sum-}(R)$, i.e. the value of E_{tE+H}^{sum-} taken in analogy with (5) for $i \in R$, to $E_{tECAL}^{5\times5}$:

$$F_{E+H}(R) = E_{tE+H}^{sum-}(R)/E_{tECAL}^{5\times5}. \tag{7}$$

Its dependence on the distance from the center of gravity $R(\eta, \phi)$ (counted from the most energetic ECAL crystal cell) is shown in Fig. 13 by solid lines. This variable also reaches its saturation in the same range of $R(\eta, \phi) \approx 0.3 - 0.4$. The difference between solid and dashed curves defines the percentage of transverse energy deposited by electromagnetic showers produced by charged pions from the η meson decay in ECAL cells around the 5×5 ECAL crystal window containing γ^{dir}-candidate with $E_{tECAL}^{5\times5} \geq 35~GeV$. This difference does not exceed $14 - 20\%$ in Barrel and $7 - 9\%$ in Endcap. Its dependence on the distance in the region of small $R(\eta, \phi)$ is evident from these pictures.

Multiplying the values of the ratios $F_H(R)$ and $F_{E+H}(R)$, in the region where they reach their saturation, by $E_{t\,ECAL}^{5\times5}$ one can obtain E_t mean values of the corresponding distributions on the plots of Figs. 11 and 12 (with the RMS values pointed on the plots).

Up to now we have been discussing the charged decay channels of the η meson alone. As for the $\omega \to \pi^+\pi^-\pi^0$ and $K_s^0 \to \pi^+\pi^-$ decays, let us note that the former is analogous to $\eta \to \pi^+\pi^-\pi^0$ decay (even a bit easier from the viewpoint of rejection because the value of the charged pion deflection in angles θ and ϕ from the π^0 direction is, on the average, twice larger). The channel $K_s^0 \to \pi^+\pi^-$ does not have a neutral particle. In this case the probability that no signal in the HCAL will be observed after imposing the cut $Et_{ECAL}^{5\times5} \geq 35\ GeV$ is very small [7].

Thus, we can conclude that to suppress contributions from the meson decays via charged channels one can impose the upper cuts

- on the value of E_t deposited only in the HCAL in the isolation cone of the radius of $R_{isol}^\gamma = 0.3$ for Barrel as well as for Endcap (according to dashed lines in Fig. 13). We can require that $E_{t\,H}^{sum} \leq E_{t\,H}^{thr}$. The value of the threshold $E_{t\,H}^{thr}$ depends on the parent meson E_t. We choose this cut to be equal to $0.5 - 1\ GeV$ for $E_t^\gamma = 40\ GeV$, gradually increasing to $E_{t\,H}^{thr} = 2\ GeV$ for $E_t^\gamma = 200\ GeV$ (see left-hand plots of Figs. 11 and 12).

- on the value of E_t deposited in the calorimeter "ECAL+HCAL" cells within the radius of $R_{isol}^\gamma = 0.3$ beyond the 5×5 ECAL window. We can require that $E_{t\,E+H}^{sum-} \leq E_{t\,E+H}^{thr}$ (with $E_{t\,E+H}^{thr} = 2 - 5\ GeV/c$) in accordance with the right-hand plots of Figs. 11 and 12. These values justify our choice of absolute isolation cut in [3] [8].

Therefore, we see that the two criteria introduced above may allow the charged hadronic decay channels of η, ω and K_s^0 mesons to be suppressed with a good efficiency (about 98%, depending on the exact value of $E_{t\,E+H}^{thr}$; see Figs. 11 and 12).

We have considered above the extreme case of the single meson decaying through charged channels. Certainly, those criteria would be much more efficient in the case of real pp collisions where η, ω and K_s^0 mesons may have a hadronic accompaniment in the isolation cone around them.

To conclude let us add that these criteria can be strengthened while selecting the "$\gamma + jet$" events in real pp collisions where they can be supplied by an additional requirement of an absence of a charged particle track with $E_t > 1\ GeV$ within the isolation cone of radius $R_{isol}^\gamma = 0.7$ around a photon candidate in the opposite (in ϕ)

---

[7] and it is defined by the probability of the case when both charged pions deposit their energies in ECAL only

[8] About $65 - 70\%$ of the signal events with direct photon satisfy this requirement (see [7]).
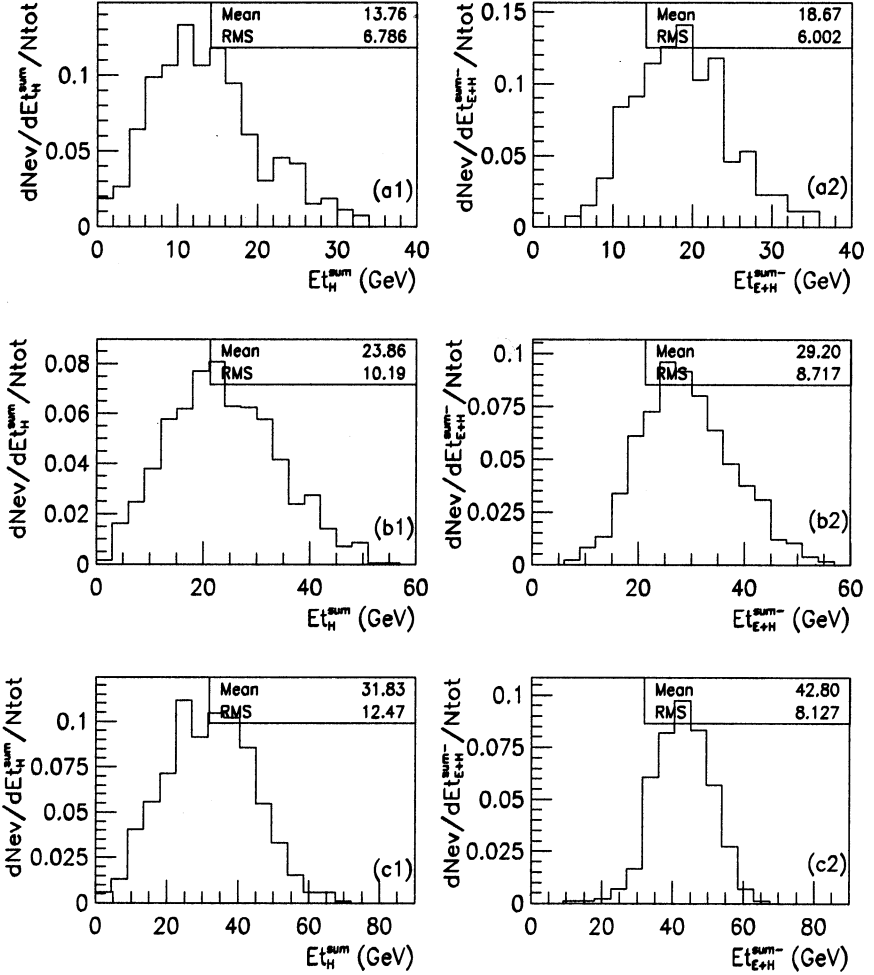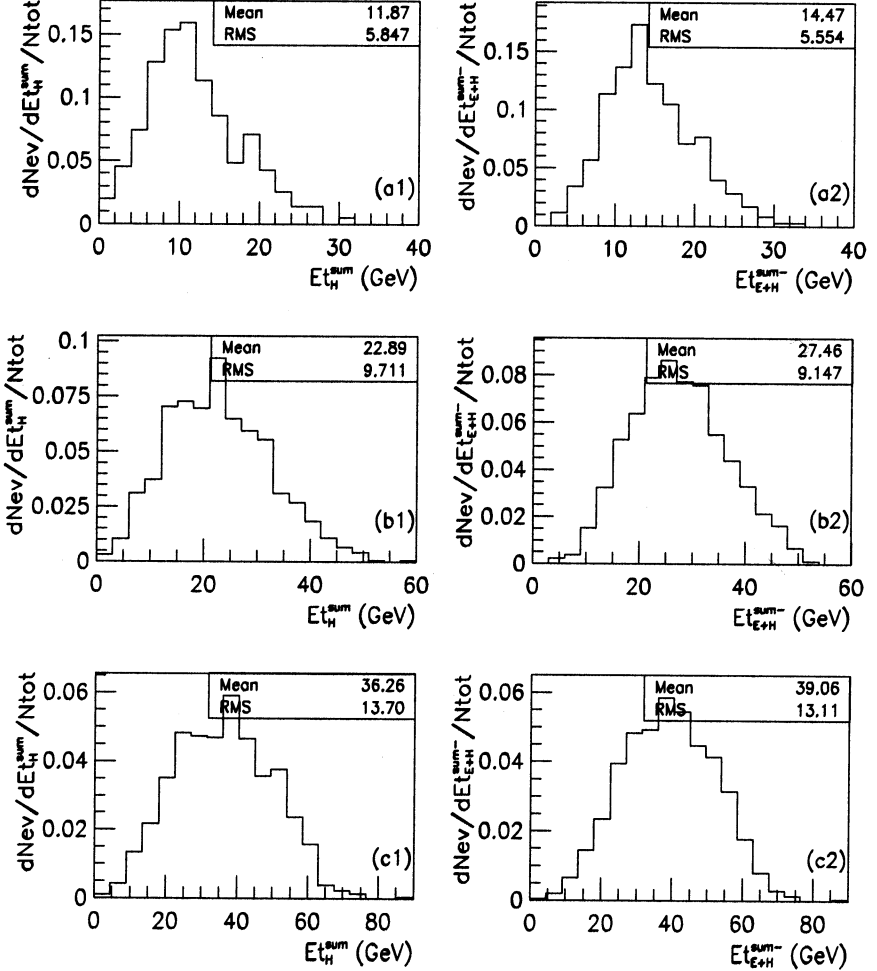
Figure 11: Normalized distributions of number of the η meson charged decay events over E_t deposited within the radius $R(\eta, \phi) = 0.7$, counted from the most energetic ECAL crystal cell, (1) in HCAL (a1, b1, c1) and (2) in "ECAL+HCAL" cells beyond the ECAL 5×5 crystal cell window (a2, b2, c2). The 1st row (a1, a2) corresponds to the initial E_t of the η meson in the range $40 \leq E_{t\,init}^{\eta} \leq 60\ GeV$, the 2nd row to that in the range $60 \leq E_{t\,init}^{\eta} \leq 80\ GeV$ and the 3rd to that in the range $80 \leq E_{t\,init}^{\eta} \leq 100\ GeV$. All distributions were obtained with the cut $E_{t\,ECAL}^{5\times5} \geq 35\ GeV$. The Barrel case ($\eta = 0.4$).

14

Figure 12: Normalized distributions of number of the η meson charged decay events over E_t deposited within the radius $R(\eta, \phi) = 0.7$, counted from the most energetic ECAL crystal cell, (1) in HCAL (a1, b1, c1) and (2) in "ECAL+HCAL" cells beyond the ECAL 5×5 crystal cell window (a2, b2, c2). The 1st row (a1, a2) corresponds to the initial E_t of the η meson in the range $40 \leq E_{t\,init}^{\eta} \leq 60 \; GeV$, the 2nd row to that in the range $60 \leq E_{t\,init}^{\eta} \leq 80 \; GeV$ and the 3rd to that in the range $80 \leq E_{t\,init}^{\eta} \leq 100 \; GeV$. All distributions were obtained with the cut $E_{t\,ECAL}^{5 \times 5} \geq 35 \; GeV$. The Endcap case ($\eta = 1.7$).

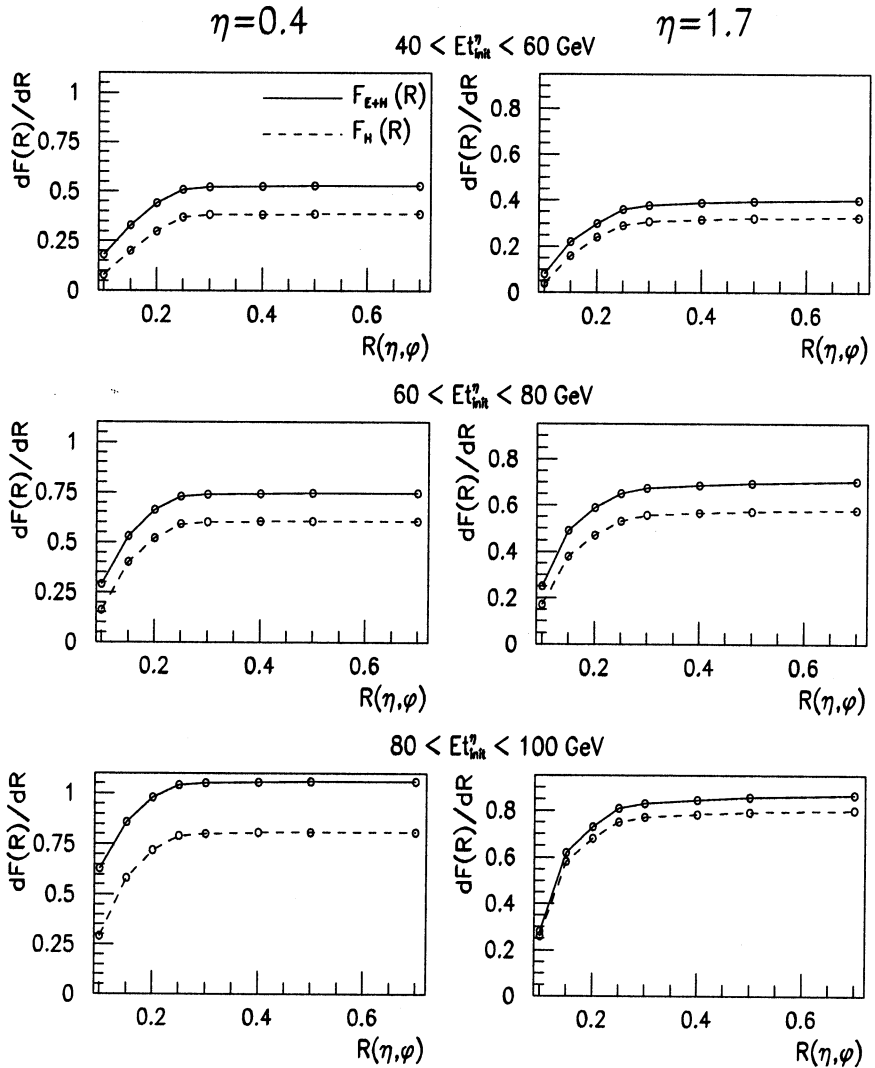Figure 13: Distributions of the ratios of the E_t deposited in HCAL (dashed line) and in "ECAL+HCAL" cells beyond the ECAL 5×5 crystal cell window (solid line) to the E_t deposited inside this window as the function of the distance from the center of gravity $R(\eta, \phi)$, counted from the most energetic ECAL crystal cell. Left-hand and right-hand columns correspond to the Barrel ($\eta = 0.4$) and Endcap ($\eta = 1.6$) cases.

direction to a jet (see also [3], [7]). The additional rejection of the charged pions that do not reveal themselves in HCAL below some threshold depends mainly on the track finding efficiency for them.

References

[1] N.B. Skachkov, V.F. Konoplyanikov D.V. Bandourin, "Photon – jet events for calibration of HCAL". Second Annual RDMS CMS Collaboration Meeting. CMS-Document, 1996–213. CERN, December 16-17, 1996, p.7-23.

[2] N.B. Skachkov, V.F. Konoplyanikov D.V. Bandourin, "γ-direct + 1 jet events for HCAL calibration". Third Annual RDMS CMS Collaboration Meeting. CMS-Document, 1997–168. CERN, December 16-17, 1997, p.139-153.

[3] D.V. Bandourin, V.F. Konoplyanikov, N.B. Skachkov. "Jet energy scale setting with "$\gamma + jet$" events at LHC energies. "Jet energy scale setting with "$\gamma + jet$" events at LHC energies. Generalities, selection rules." JINR Preprints E2-2000-251, JINR, Dubna, hep-ex/0011012.

[4] D.V. Bandourin, V.F. Konoplyanikov, N.B. Skachkov. "Jet energy scale setting with "$\gamma + jet$" events at LHC energies. Event rates, P_t structure of jet." JINR Preprints E2-2000-251, JINR, Dubna, hep-ex/0011013.

[5] D.V. Bandourin, V.F. Konoplyanikov, N.B. Skachkov. "Jet energy scale setting with "$\gamma + jet$" events at LHC energies. Minijets and cluster suppression and $P_t^{\gamma} - P_t^{Jet}$ disbalance." JINR Preprints E2-2000-252, JINR, Dubna, hep-ex/0011084.

[6] D.V. Bandourin, V.F. Konoplyanikov, N.B. Skachkov. "Jet energy scale setting with "$\gamma + jet$" events at LHC energies. Selection of events with a clean "$\gamma + jet$" topology and $P_t^{\gamma} - P_t^{Jet}$ disbalance." JINR Preprints E2-2000-253, JINR, Dubna, hep-ex/0011014.

[7] D.V. Bandourin, V.F. Konoplyanikov, N.B. Skachkov. "Jet energy scale setting with "$\gamma + jet$" events at LHC energies. Detailed study of the background suppression." JINR Preprints E2-2000-251, JINR, Dubna, hep-ex/0011017.

[8] D.V. Bandourin, V.F. Konoplyanikov, N.B. Skachkov, " "$\gamma + jet$" events rate estimation for gluon distribution determination at LHC", Part.Nucl.Lett.103:34-43,2000, hep-ex/0011015.

[9] P. Aurenche *et al.* Proc. of "ECFA LHC Workshop", Aachen, Germany, 4-9 Oktob. 1990, edited by G. Jarlskog and D. Rein (CERN-Report No 90-10; Geneva, Switzerland. 1990), Vol. II.

[10] M. Dittmar, F. Pauss, D. Zurcher, Phys.Rev.D56:7284-7290,1997.

[11] M. Dittmar, K.Mazumdar, N. Skachkov, Proc. of "CERN Workshop on Standard Model Physics (and more) at the LHC", QCD, Section 2.7 "Measuring parton luminosities ...", Yellow Report CERN-2000-004, 9 May 2000, CERN, Geneva.

[12] A. Kyriakis, D. Loukas, J. Mousa, D. Barney, CMS Note 1998/088, "Artificial neural net approach to $\gamma - \pi^0$ discrimination using CMS Endcap Preshower".

[13] Particle Data Group, D.E. Groom *et al.*, The European Physical Journal C15 (2000) 1.

[14] GEANT-3 based simulation package of CMS detector CMSIM. CMS TN/93-63, C. Charlot *et al*, "CMSIM–CMANA. CMS Simulation facilities", CMSIM User's Guide at WWW: http://cmsdoc.cern.ch/cmsim/cmsim.html.

[15] D. Barney, P. Bloch, CMS-TN/95-114, "π^0 rejection in the CMS endcap electromagnetic calorimeter - with and without a preshower."

[16] CMS Electromagnetic Calorimeter Project, Technical Design Report, CERN/LHCC 97–33, CMS TDR 4, CERN, 1997.

Бандурин Д. В., Конопляников В. Ф., Скачков Н. Б.   Е1-2001-261

О возможности разделения π^0-, η-, ω-, K_s^0-мезонов и фотона
по калориметрической информации в CMS-детекторе

Анализируется возможность разделения фона от π^0-, η-, ω- и K_s^0-мезонов
и сигнала от фотонов, рожденных непосредственно в pp-столкновениях.
На основании только калориметрической информации вычислены коэффи-
циенты режекции для двух интервалов по псевдобыстроте $0{,}4 < \eta < 1{,}0$ и
$1{,}6 < \eta < 2{,}0$ и шести значений E_t, равных 20, 40, 60, 80, 100 и 200 ГэВ. Случаи
с η-, ω- и K_s^0-мезонами, распадающимися по нейтральным и заряженным кана-
лам, рассмотрены отдельно.

Bandourin D. V., Konoplyanikov V. F., Skachkov N. B.   Е1-2001-261

On the Possibility of Discrimination between π^0-, η-, ω-,
K_s^0-Mesons and a Photon Based on the Calorimeter Information
in the CMS Detector

The possibility of π^0-, η-, ω- and K_s^0-mesons background separation
from the signal photons produced directly in pp collisions is analyzed. The rejec-
tion factors for two pseudorapidity regions $0.4 < \eta < 1.0$ and $1.6 < \eta < 2.0$ and six
E_t values, equal to 20, 40, 60, 80, 100 and 200 GeV, are calculated for a case
when only the calorimeter information is used. The cases of η-, ω- and K_s^0-mesons
decaying through neutral and charged channels are considered separately.